DuraCap: a Power-Bootstrapping, Maximum Power Point Tracking Energy-Harvesting System

Chien-Ying Chen
Directed by Prof. Pai H. Chou

National Tsing-Hua University, Taiwan
Embedded Platform Lab
dogs007.tw@gmail.com

July 12, 2009

Contents

List of Figures

List of Tables

Abstract

DuraCap is a solar-powered energy harvesting system that stores harvested energy in supercapacitors and is volage compatible with lithium-ion batteries. The use of supercapacitors instead of batteries enables DuraCap to extend the operational life time from tens of months to tens of years. DuraCap addresses two additional problems with micro-solar systems, namely cold booting and maximum power point tracking (MPPT). Cold booting is when the system starts running from the state of total exhaustion of stored energy, and it can be inefficient due to the long charging time of supercapacitors. We solve this problem by dedicating a smaller supercapacitor to this stage before handing over to the array of larger-value supercapacitors. To enable accurate and efficient MPPT, we propose and evaluate a bound-control circuit for PFM regulator switching. The DuraCap also contains an I-V tracer to obtain the I-V curve and P-V curve of the solar panel to enable self-configuring to match solar panels of different types and sizes. Two types of enhanced switch for power path switching are designed for low voltage control that reduces the power consumption. Experimental results show the DuraCap's bound-control MPPT circuit, enhanced switch, and supercapacitor array achieve the highest conversion efficiency, thereby enabling low power consumption and long operational life time.

Chapter 1

Introduction

The energy is one of the greatest limiting factors on the operating lifetime of wireless sensor networks. Sensor nodes often use batteries as the only energy source that requires maintenance by the user over time. To overcome these limitations, an energy harvesting system that provides durable power for wireless sensing systems is needed.

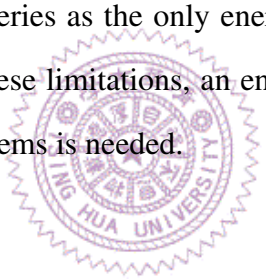

1.1 Problem Statement

The goal of our work is to develop a solar-powered, high-capacity, maximum power point tracking energy harvesting system. This thesis assumes that the target device is a platform for applications in a wireless sensor network deployed in an outdoor environment. This thesis also specifically assumes the energy source to be sunlight, which is converted into electricity by a solar panel that is rated to produce over $300mW$ of power. The final assumption is that the energy harvesting system contains a microcontroller to either manage the power path switching on the system or perform MPPT for the solar panel.

1.2 Requirements and Objectives

Self-Recovery

Since the DuraCap uses sunlight as the energy source, the input power is directly influenced by the weather condition. The system collects energy and charges the supercapacitor when the sunlight is available. At night, the system draws power from the supercapacitor array to the target device. However, the weather may not be stable, and the system may exhaust all of its energy stored in the supercapacitors if sunlight is blocked for an extended period of time. In that case, the system goes into dead state. Since the system may be deployed in the wild, it must be able to recover from the dead state, a process we call *cold booting*.

Another situation that requires cold booting capability is when the system is booting up for the first time, i.e., before the system has a chance to configure the energy-harvesting circuitry. The DuraCap requires no configuration during the first boot. In fact, there is no difference between booting for the first time and cold booting from dead state. The DuraCap is intended for providing durable, stable power service for the target device, and thus the user can concentrate on the development of the target device and application.

Maximum Power Point Tracking

The DuraCap uses a solar panel as the energy harvesting device. It is well known to behave as a current source with a voltage limiter. To get high harvesting efficiency, the DuraCap must adjust the load to match the solar panel's specific operating point called the *maximum power point*. The technique to track the maximum power point of the solar panel for the energy harvesting system is well known as *maximum power point tracking* (MPPT). It is evident that harvesting efficiency is much higher when MPPT is performed on the solar panel[16]. In this thesis, the DuraCap has multiple modes of performing MPPT in order to keep the harvesting efficiency high in variety of

environments.

Power Consumption

Power consumption is one of the most important points in designing an energy harvesting system. It includes power consumption on power path switching circuit, MPPT circuit, system controller, and energy loss due to regulator conversion. Less power consumption means more energy can be delivered to the target device, and thus the power consumption of the system should be controlled to be as low as possible. Moreover, a smaller-sized energy source device provides less energy to the system due to the physical size restriction mentioned above. The power consumption must be lower than the power level that can be delivered by the energy source.

Size Constraint

The DuraCap is designed for embedded systems such as wireless sensor nodes and hand-held computers. Most of these systems are constrained on size due to their application requirements. To fit the size of the target system, systems that include energy harvesting should especially be as small as possible. However, a smaller energy conversion device tends to produce less available power than a larger one. Thus, the energy conversion device should be considered between physical size and energy productivity.

Operating Voltage Range

A solar panel can have a wide voltage range, especially if internally it is composed of several panels in series. To operate for most commercially off-the-shelf, consumer-grade solar panels, the circuit and components of the system must be able to handle relative high voltage from solar panel compared to the system voltage level. In this thesis, the system voltage should be as low as possible

in order to reduce the power consumption, at a much lower than the voltage of the solar panel.

1.3 Contributions

In this thesis, we develop several ideas on solar-powered energy harvesting into an actual system named DuraCap. It provides durable power for wireless sensor networks to extend the operational life time from several months to possibly tens of years. A bound-control PFM regulator controller for MPPT has been developed. It enables the system to maintain the solar panel generating the maximum power while the microcontroller stays in the sleep mode. An enhanced switch for the PFM regulator and a power path switch for the supercapacitor array are designed for low-voltage control, which helps the system reduce power consumption. Several MPPT approaches have been implemented and validated on the DuraCap. Experimental results show that the DuraCap uses bound-control MPPT circuit, the enhanced switch, and the supercapacitor array to achieve high conversion efficiency, low power consumption, and long operational life time.

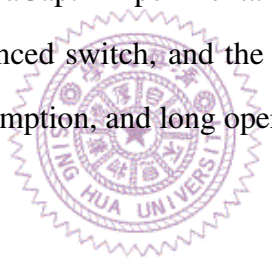

Chapter 2

Background and Related Work

2.1 Energy Source

Ambient Sources

Many ambient energy sources have been proposed, including solar radiation, vibration, thermal differential, water flow, and wind. These sources produce energy in different ways, and all of those sources have operational restrictions caused by the operating environment. Despite these restrictions, ambient energy sources provide free, clean and durable power, and sometimes it may be the only viable choice for long-term or remote deployments.

In this thesis, the DuraCap energy harvesting system is designed for the wireless sensor node

Table 2.1: Comparison between power density [13]

Energy Source	**Harvesting Technology**	**Power Density**
Solar radiation	Solar Cells (outdoors at noon)	$15mW/cm^3$
Pressure	Piezoelectric (shoe inserts)	$330\mu W/cm^3$
Vibration	Small microwave oven	$116\mu W/cm^3$
Heat	Thermoelectric (10°C gradient)	$40\mu W/cm^3$
Voice	Acoustic noise (100dB)	$960nW/cm^3$

that are deployed in an outdoor environment. The objectives include small size and high conversion efficiency. The smaller size means lower power output, and this makes conversion efficiency even more important.

The most popular ambient energy source is solar radiation, and manufacturing techniques for solar panels have improved from both physical size and conversion efficiency in recent years. Moreover, solar panels have the highest power density among all harvesting techniques [4], as shown in Table 2.1 for some energy sources [13].

According to factors in cost, energy conversion efficiency, size, power density, and the operating environment, solar panels make the best choice for the class of applications evaluated in this thesis.

Solar Panel

A solar panel consists of several *solar cells*, which are also known as *photovoltaic cells*. A solar cell is a silicon device that converts light energy into electricity. A solar cell reacts to different light sources, such as artificial light and the light from sun. However, the conversion efficiency is calculated based on the optical spectrum of the light source. Although artificial light sources are readily available from indoor surroundings, such as fluorescent and incandescent lights, their narrower optical spectrum leads to lower energy conversion efficiency of the solar cell. The light source is specifically to be the sunlight because the solar radiation contains *total spectrum of the electromagnetic radiation* , excites more electricity from the solar cell due to the principle of working. According to the principle, the stronger sunlight the solar cell captured, the more electrical power is produced. This thesis assumes the target device is to be deployed in an outdoor environment where the sunlight is sufficient to support the target device, thus the system should be able to obtain durable energy from the solar panel.

The sunlight intensity is greatly influenced by the changing weather, which causes the output

power of the solar panel to vary in a wide dynamic range. Since the output power is not constant, and the solar panel is well known to behave as a current source with a voltage limiter, it is very important to operate the load in a specific point to obtain the maximum power from the solar panel.

The open-circuit voltage and short-circuit current values of the solar panel are concerned with the sunlight intensity.

2.2 Energy Storage

An energy storage element stores electrical energy converted by the solar panel. It is one of the most important elements in many energy harvesting systems, even though some exclude storage by delivering the harvested power to the target system directly. In this thesis, we consider applications that require a long, continuous time of operation including night time without sunlight. Therefore, the system needs more than one energy storage element.

The two common types of energy storage for energy harvesting systems are batteries and supercapacitors. Their trade-offs are discussed in the following subsections.

Batteries

A battery is a common energy storage device that stores energy in a chemical form. Most commercial electronic products use rechargeable battery because it is a mature storage technology. Several types of rechargeable batteries to be considered include lithium-ion, nickel metal hydride (NiMH), nickel cadmium (NiCd), and nickel-iron. Some designs have been presented to use rechargeable batteries for their energy harvesting systems [8].

Supercapacitors

Supercapacitors, also known as *electrochemical double layer capacitors* (EDLCs), or *ultracapacitors*, have been proposed for many applications in recent years [18], including energy harvesting systems. Supercapacitors behave just like common capacitors but have much higher capacitance. Several designs incorporate supercapacitors into their energy harvesting systems [2, 1, 16, 17, 5].

Comparison between Batteries and Supercapacitors

Both rechargeable batteries and supercapacitors can make a good choice for energy harvesting systems. The designer should consider the following factors.

- Power Density vs. Energy Density

  The *power density* of an energy storage device refers to the instantaneous maximum output power level. The *energy density* means the amount of stored energy per unit volume. Batteries have relatively high energy density but relatively low power density, while supercapacitors have lower energy density but a relatively high power density [13]. In other words, supercapacitors cannot stores as much energy but can output a higher level of power instantaneously than battery [4].

- Charge Rate and Discharge Rate

  The charge/discharge rate of the battery is much smaller than the supercapacitor since the battery is a chemical energy storage device. Besides, the power density of the supercapacitor is much greater than the battery as mentioned above, and thus the supercapacitor can be charged with a higher current and has a shorter charge time.

- Life Time

  The energy storage capacity decreases as the number of recharge cycles increases. For most

common batteries, the recharge cycle life time is limited to 10^3 cycles. For supercapacitors, the recharge cycle life time is as many as 10^6 cycles [6]. It is obviously that the life time of supercapacitors is much greater than that of batteries.

- Self-discharge Rate

  Both batteries and supercapacitors have a self-discharge effect, which is also called leakage. The energy stored in the battery or supercapacitor drops even if no load is connected. The self-discharge effect of the battery is divided into two stages: the first 24 hours and the time after that. The self-discharge rate of the battery for the first 24 hours is 5% in general, and then it turns into 1% to 2% per month after that [14]. It is a relatively small value compared to that of supercapacitors, up to 30% per week [6]. However, in this thesis we assume that the energy stored in the storage device is consumed within two days. For this reason, the term self-discharge rate could be neglected.

- Voltage

  For the energy harvesting system, it is important to understand the voltage of the energy storage device. A common one cell lithium-ion battery has an open-circuit voltage range of 3.7V to 4.2V. In contrast with batteries, supercapacitors have a voltage range in the range of 0V to 2.7V.

- Energy Measurement

  The energy harvesting system measures the energy storage device, so that it is able to decide the system status, hence estimating the charging time and the rest available energy in the system. Since the voltage drop of the battery is not linear, it is difficult to monitor its remaining energy without using a battery fuel gauge, which incurs extra cost and power consumption. In contrast, the voltage drop of the super-capacitor is linearly proportional to the discharged energy, and therefore the system can monitor the remaining energy by measuring the voltage directly.

Table 2.2: Comparison between Batteries and Supercapacitors.

	Battery	**Supercapacitor**
Recharge Cycle Life Time	10^3 cycles	10^6 cycles
Self-discharge Rate	5%[a]	30%
Voltage	3.7V-4.2V[b]	0V-2.7V
Energy Density	high	low
Power Density	low	high
Charge/Discharge Rate	low	high

[a] *Self-discharge rate of lithium-ion battery in the first 24 hours.*
[b] *One cell lithium-ion battery.*

Table 2.2 shows a comparison between batteries and supercapacitors. Supercapacitors have advantages that are important for the design in this thesis. Our system is designed to supply multiple power outputs in different voltage level , and each power output is supplied by a single storage device at a time. To do this, multiple energy storage devices are used, and the storage device must be charged in a short time. Moreover, the storage device must be able to withstand a large number of charging and discharging cycles since it could be multiple cycles in a single day, or thousands of cyclein a year. Besides, this thesis assumes the energy is consumed within two days, and thus the self-discharge effect can be ignored.

For these reasons, we choose a supercapacitor over a battery for the energy harvesting system in this thesis.

2.3 Energy Harvesting Systems

Solar energy harvesting systems have emerged as a consumer product in recent years. Most of solar energy harvesting systems perform MPPT [3, 7, 15] to increase the power conversion efficiency.

Heliomote

Heliomote [8] is a wireless sensor node that uses solar panels as its energy source. Two AA-type NiMH batteries are used as the only energy storage in the system. In the Heliomote, the solar panel connect to the batteries directly through a protection diode without any MPPT circuit. This solution reduces the efficiency of charging, since the operating point of the solar panel in $V_{BAT} + 0.7$ is much lower than the maximum power point. Besides, the system begins charging only when the solar panel voltage is higher than $V_{BAT} + 0.7$. As a consequence, the amount of charging power drawn from the solar panel depends on the remaining energy level of the battery.

Prometheus

Prometheus[5] uses both a supercapacitor and a Li-Polymer battery as its power buffers. The solar panel first charges the supercapacitor while sufficient power is available from the solar panel. The system then charges the battery when the supercapacitor voltage is higher than a certain threshold. While the solar panel does not output sufficiently high power, it draws power from the supercapacitor first, with the goal of avoiding drawing power from the battery unless absolutely necessary. This feature is expected to increase the lifetime of the battery. Similar to Heliomote, Prometheus connects both a supercapacitor and a battery to the solar panel directly, and thus it has the same drawbacks in using the solar panels as Heliomote.

AmbiMax

AmbiMax [2] is a simple and low-cost energy harvesting system that performs maximum power point tracking. AmbiMax accepts two types of ambient energy sources: solar panel and wind generator. It uses only low-power logic components instead of containing a microcontroller or any programmable devices. The MPPT circuit is built with a hysteresis comparator that uses a

photosensor as the reference signal. Although it consumes very low power, the system requires the presence of a battery as secondary power source when supercapacitors are empty.

Solar Energy Harvester with Pilot-Cell

This energy harvesting system [1] uses the architecture based on the AmbiMax with part modifications. One main difference from AmbiMax is that this system proposes a small P-V module as a reference input for MPPT instead of a photosensor. This small P-V module, also called the *pilot-cell*, actually is a small solar panel that outputs a few hundred millivolts maximum. It is important that the pilot-cell be selected carefully to closely represent the characteristics of the main solar panel. The operating point of the pilot-cell follows almost linearly the behavior of the main solar panel during light variations. The pilot-cell provides feedback information for the MPP tracker to control the regulation of the MPP regulator. The advantage of using the pilot-cell is that the reference input does not require any additional power, whereas Ambimax's photosensor consumes power all the time.

Like AmbiMax, Everlast, and Prometheus, this system uses a supercapacitor as a power buffer. However, the supercapacitor is not indispensable since the system is able to choose automatically the power source between the solar panel and the DC-DC converter. As the power supplying from the solar panel, the system guarantees faster recovery from an empty energy status.

Everlast

Everlast [16, 17] is a wireless sensor node with a built-in solar MPPT system that uses a supercapacitor as its only energy storage. Everlast performs MPPT on the same microcontroller as the sensor node's to execute an MPPT algorithm and drives a series of pulses to control the PFM (pulse-frequency modulation) regulator. An I-V tracer is presented to tracking the maximum power point of the solar panel in a constant-interval time. The harvesting efficiency of the Ever-

last is much higher than Heliomote and Prometheus. However, the software MPPT requires the microcontroller to stay active all the time, and this potentially consumes more power.

Chapter 3

DuraCap System Design

3.1 System Overview

DuraCap consists of several parts: solar panel, energy storage, system control unit, power regulator, and MPPT circuitry. The goal of DuraCap is to harvest energy from a solar panel in an efficient way and maintain durable power for the target device. DuraCap is designed to be a standalone system, which means that the users are able to use this system without any configurations. Meanwhile, DuraCap provides a 4.2V output, which is similar to a Li-Ion battery, and thus the users can easily replace the battery with a DuraCap system without any changes to the target device.

Fig. 3.1 shows the system block diagram of the DuraCap. The following sections describe concerns and details for designing DuraCap.

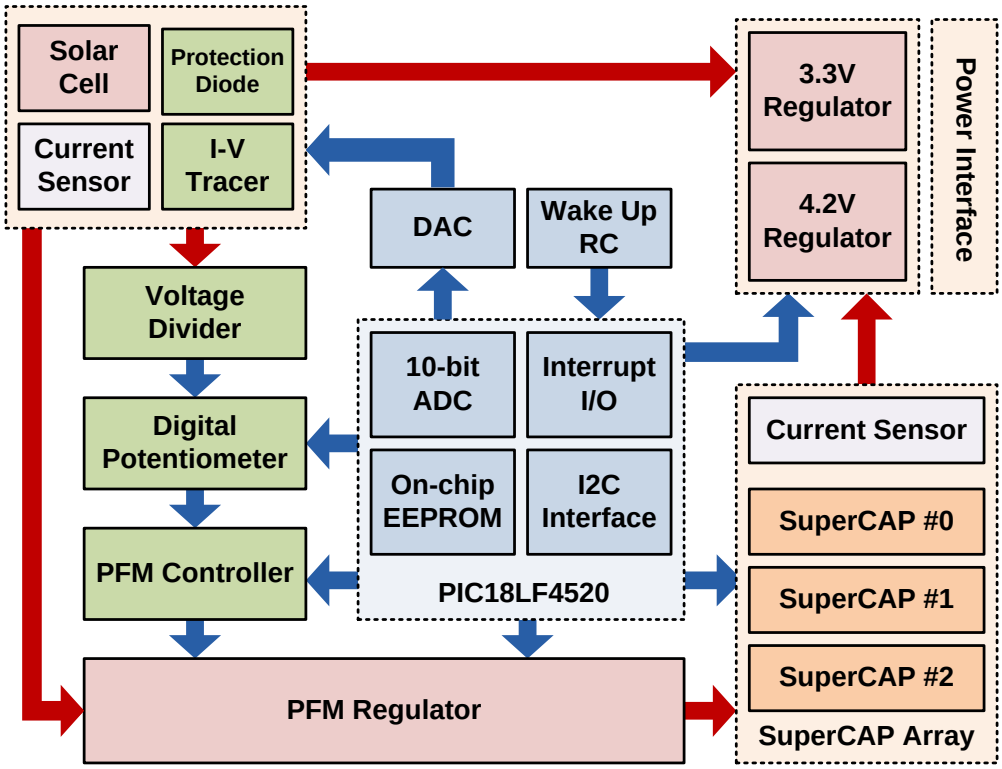

Figure 3.1: DuraCap system block diagram.

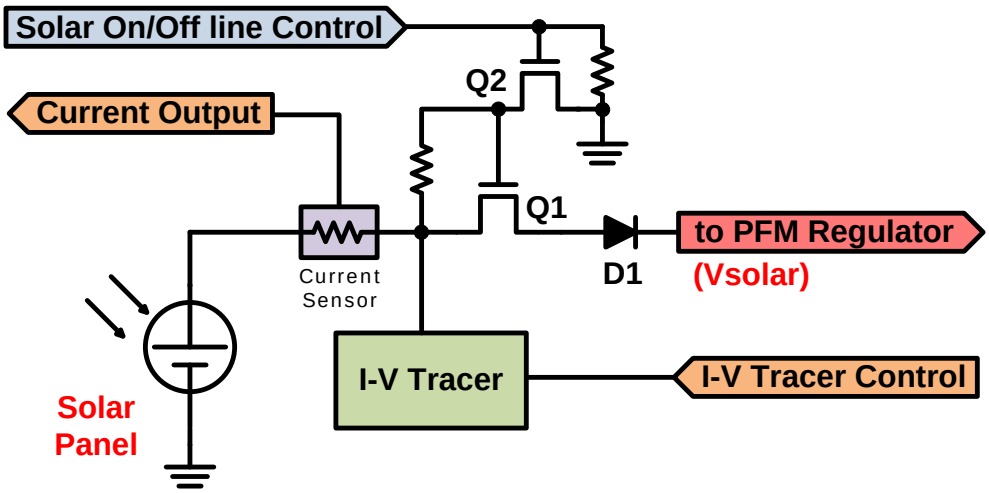

Figure 3.2: The circuit around the solar panel.

3.2 System Detail

3.2.1 Solar Panel and Protection

The solar panel captures sunlight and converts it into electrical power. It has a wide voltage range due to the variety of weather. When the sunlight is available and strong enough, the solar panel produces energy and acts as a power supplier of the system. However, when the solar panel cannot get enough light, the output voltage of the solar panel drops to a very low voltage, and the solar panel may be damaged by the adverse current from the system. To protect solar panels from the adverse current damage, a diode is added between solar panel and the system, as shown as $D1$ in Fig. 3.2.

Moreover, a group of MOSFETs, $Q1$ and $Q2$ in Fig. 3.2, are added between the solar panel and the protection diode to build a solar panel on/off line switch. The solar panel on/off line switch provides standalone control function for the system. By controlling this switch, the system can isolate the solar panel from the rest of the system, thereby enabling the system to perform the I-V curve tracing.

3.2.2 Energy Storage

DuraCap uses a supercapacitor to store converted power. Three supercapacitors are used to construct a storage array that provides power-bootstrapping function for DuraCap, as shown in Fig. 3.3. One of the supercapacitor in the storage array is assigned as the *booting supercapacitor*, which has highest charging priority and relative small capacitance compared to the others. The booting supercapacitor requires small capacitance, because the DuraCap needs it to become fully charged as soon as possible if the system is executing the cold boot procedure, then the system can perform more efficient MPPT mode when supplying power from the booting supercapacitor. However, the booting supercapacitor still requires capacitance that is large enough to provide sufficient power to support the whole system for the duration.

The two other supercapacitors, which are named as reservoir supercapacitors in the DuraCap, have large capacitance, which provides power for the target device. In the case when the booting supercapacitor is exhausted, the system may switch to reservoir supercapacitors to perform MPPT and hence charge the booting supercapacitor.

The supercapacitor array is maintained by several switches that are called the *power path switches*. They are specifically designed to control power flow for charging and discharging of a supercapacitor. The detail of power path switch is discussed in section 3.2.5.

3.2.3 Power Supply

DuraCap provides two different output voltages: 3.3V and 4.2V. The 3.3V output is mainly supplied for the system, and the 4.2V is supplied for the target device. The 4.2V output voltage provides a power level similar to a Li-Ion battery, and thus many target devices can directly use the DuraCap as a power source without any changes. In some cases that the target device requires 3.3V power are also supported. At this time, the system and the target device use the same 3.3V

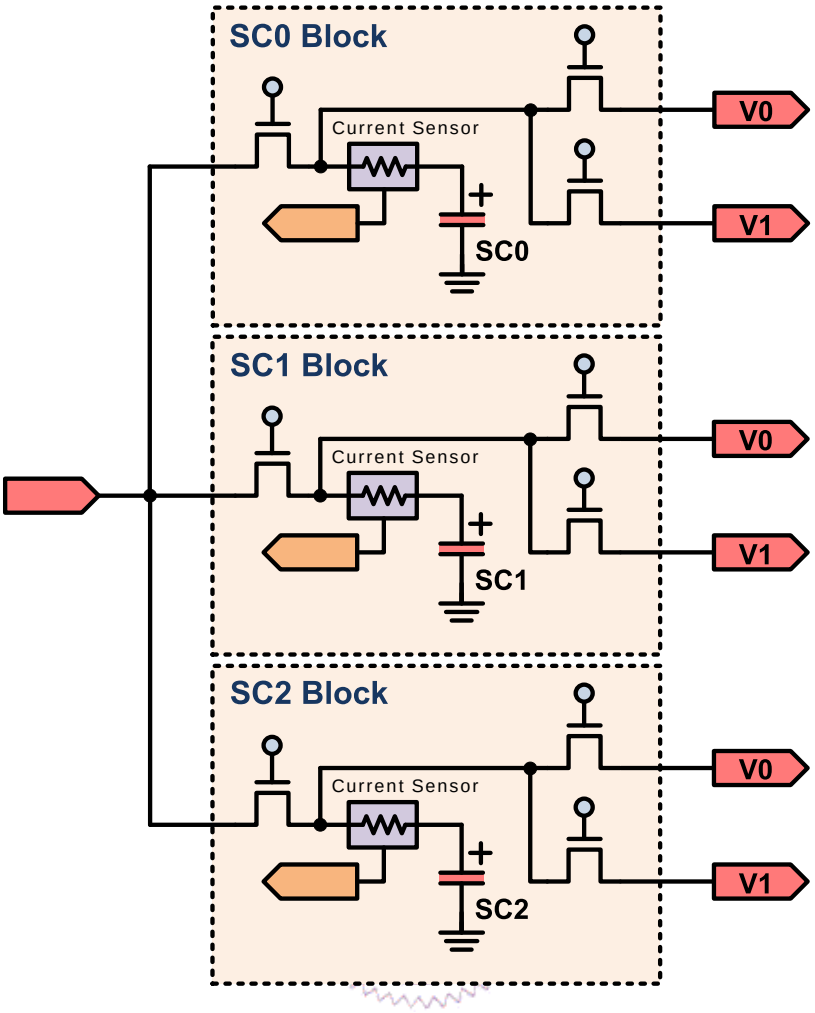

Figure 3.3: The circuit of supercapacitor array.

power output from a single regulator.

DuraCap is able to switch the input source for the regulator between solar panel and any one supercapacitor in the supercapacitor array. DuraCap always use the supercapacitor as the power source for the 4.2V regulator since the power from the solar panel is supposed to be used to support the 3.3V regulator for the system first, and then booting supercapacitor. To maintain the stable operation, the system outputs power to the target device only when more than two supercapacitors are available in the reservoir supercapacitors array.

Fig. 3.4 shows the block diagram of the power in DuraCap. Power module *PM0* and *PM1*

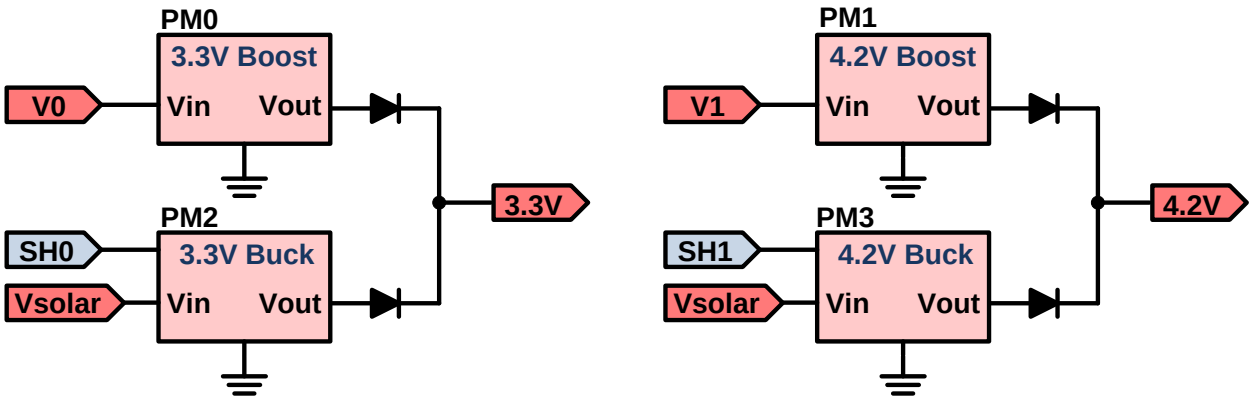

Figure 3.4: Block diagram of output power.

convert the power source from the supercapacitor array, and power module *PM2* and *PM3* convert the power source from the solar panel. Both *PM0* and *PM2* output a voltage of $3.3V$, and *PM1* and *PM3* output a voltage of $4.2V$. Most importantly, only one regulator turns on to output power at a time for each single voltage output.

3.2.4 MPPT Circuitry

PFM Regulator

The system needs a regulator to transfer the harvested energy from the solar panel to the supercapacitor. The traditional high-efficiency PWM DC-DC converter would not function properly here, because the solar panel is seen as a short to the supercapacitor when these are connected together. In DuraCap, the system uses a pulse-frequency modulated (PFM) regulator to charge the supercapacitor. By giving a series of pulse, the switch in the PFM regulator turns off PFM momentarily so that the voltage of the solar panel remains at a proper level, that is, the maximum power point.

Fig. 3.5 shows the circuit of the PFM regulator. The PFM regulator acts like a switched-capacitor circuit since it charges a capacitor and then transfers the energy to the load supercapacitor. Meanwhile, the PFM regulator is similar to a transformation of a buck regulator with the capacitor

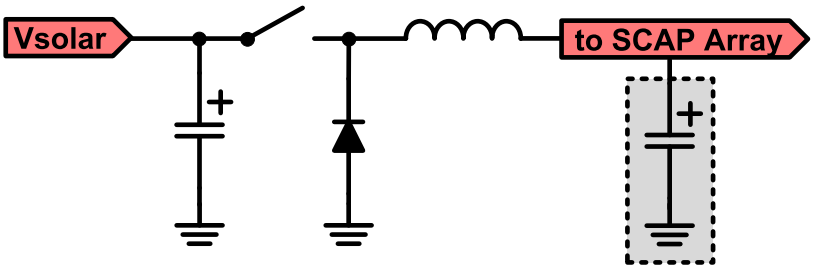

Figure 3.5: PFM regulator circuit.

moving to front side of the switch. In fact, the PFM regulator behaves as a buck regulator during the process of charging a supercapacitor. The pulse control for a PFM regulator can be either from a microntroller or a bound-control comparator (Section 3.2.4), depending on the MPPT mode in which the system is executing.

The design details of the switch in the PFM regulator is presented in Section 3.2.5.

Bound-Control PFM Switching Controller

The bound-control circuit is functionally the hardware part of bound-control MPPT mode. It gives a convenient way for the microcontroller to perform MPPT. The bound-control circuit is integrated with four common low-power comparators. Once the microcontroller gives the upper-bound and lower-bound values of the solar panel voltage, the bound-control circuit will perform switching automatically for the PFM regulator. Fig. 3.6 shows a brief circuit for bound-control circuit, where the *VR1* and *VR2* are configurable to adjust the voltage values of upper-bound and lower-bound, respectively.

Solar Panel I-V Tracer

The solar panel's I-V tracer consists of an N-type MOSFET $Q1$, the solar panel's on/off line switch $S1$, and a DAC IC, as shown in Figure 3.7. The solar panel's I-V tracer is controlled by a microcon-

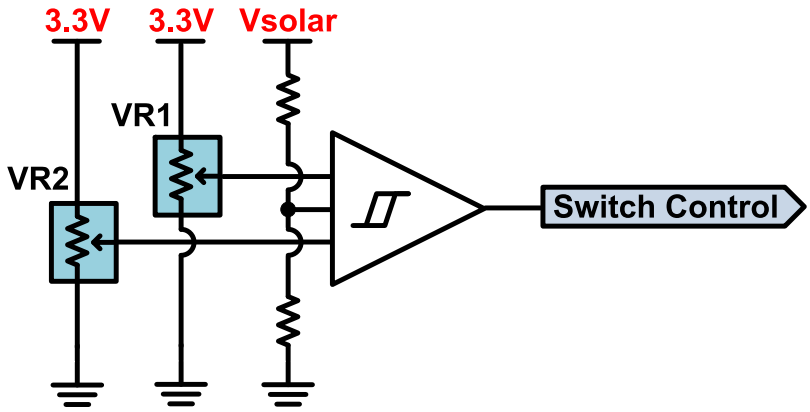

Figure 3.6: Bound-control block diagram.

troller to obtain the I-V curve of the solar panel. By tracing the I-V curve, the system can easily find the maximum power point of the dedicated solar panel, and this is how DuraCap actually accomplishes MPPT.

When performing I-V tracing for solar panels, the microcontroller disconnects the solar panel from the system momentarily by turning off the solar panel's on/off line switch. The microcontroller then operates the DAC to output a linear change of signal to the gate of the N-type MOSFET, which is much similar to varying the load on the solar panel.

Since the solar panel has to be standalone when performing I-V curve tracing, the system must source its power from the supercapacitor array instead of the solar panel. In other words, the I-V curve tracing cannot be running when the system is in a state where it must rely on the solar panel, such as during cold booting procedure or when the energy has been exhausted.

3.2.5 System Control

Enhanced Switch

To save the power consumption, the system operates at 3.3V, which is a relatively low voltage compared to the input voltage from solar panel. It can be a problem to control a high-level power

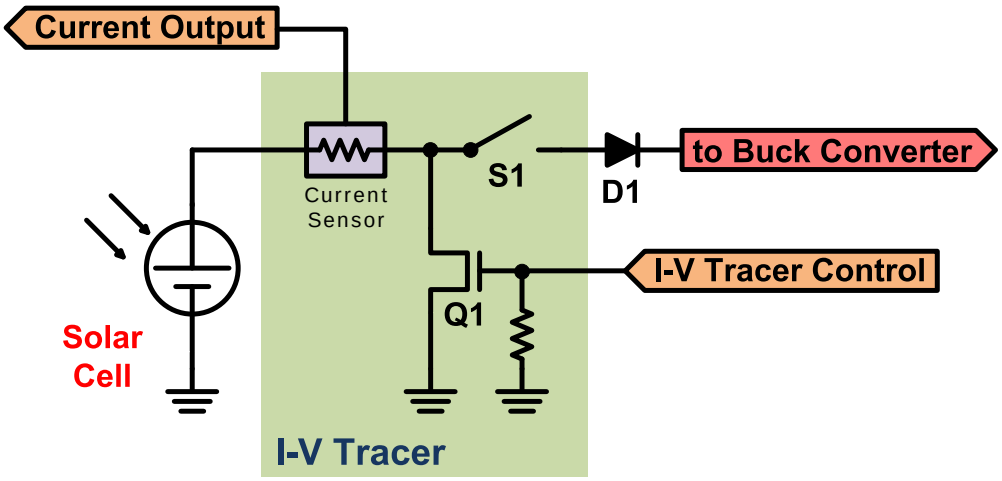

Figure 3.7: I-V Tracer Circuit.

path by using a common MOSFET from a low-level gate signal. To solve this problem, two types of enhanced switches for power path control are designed.

- Enhanced Switch for PFM Regulator

  The passing voltage to be controlled in the PFM regulator is exactly the same as the voltage of the solar panel. The switch is placed on the high side of the circuit in the PFM regulator. In general, a common P-type MOSFET is used in this case. However, it is a problem to cut the source-drain path from a relatively low voltage of the gate. Besides, the solar panel's voltage rises very slowly when the PFM regulator is working, and it causes inefficient conversion when the system is performing MPPT.

  To decrease the rising time of the solar panel, the switch must have fast response time, that is, by turning off the switch immediately. To accomplish this objective, the diode $D1$ is added into the switch as shown in Fig. 3.8.

  In Fig. 3.8, $Q1$ and $Q3$ are P-type MOSFETs, $Q2$ is an N-type MOSFET, and $D1$ is a Schottky diode. By placing a diode $D1$ between 3.3V and the P-type MOSFET $Q1$, the diode provides a short cut for raising the V_{GS} of $Q1$ starting from 3.3V, and thus the V_{GS} can

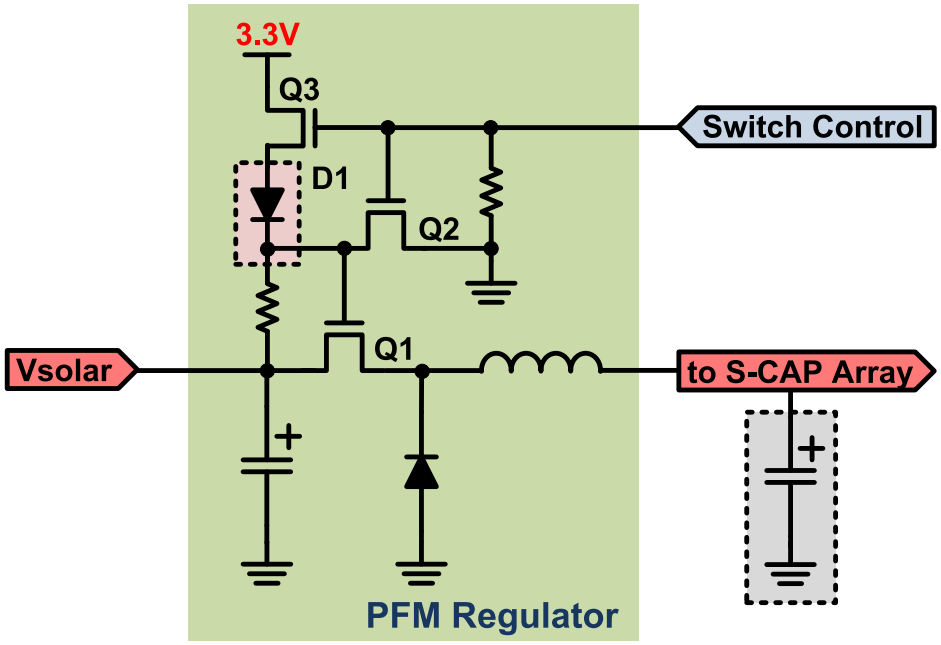

Figure 3.8: The circuit of PFM regulator with enhanced switch.

rise faster and then turn the switch off promptly.

- Power Path Switch for Supercapacitor Array

  Fig. 3.9 shows a unit block of the supercapacitor array. Three switches in Fig. 3.9 are replaced by the power path switch being discussed here.

  The objective and the problem of designing the power path switch is totally different from the enhanced switch in the PFM regulator. The power passes the power path switch here has a voltage range of 0V to 2.7V, which is the charging and discharging voltage range of the supercapacitor. Generally, a P-type MOSFET is used, since the switch is to be placed on the high side. However, if the voltage stays low most of time, then it is better to replace the P-type MOSFET by an N-type MOSFET. In order to meet both requirements, the switch is constructed with two parts of MOSFET to provide two ways for power passing.

  Fig. 3.10 shows the circuit of the power path switch for the supercapacitor array, where $Q1$ and $Q3$ are N-type MOSFETs and $Q2$ is a P-type MOSFET. When the gate control goes high,

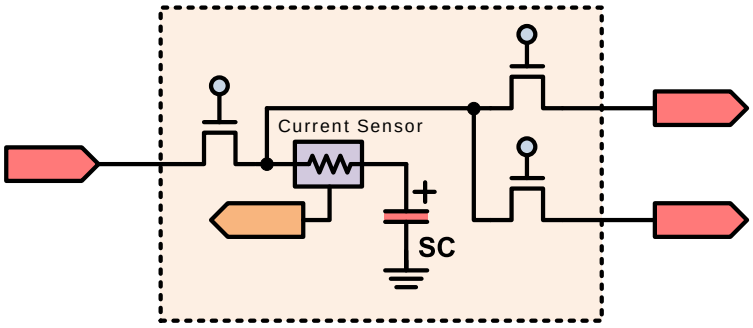

Figure 3.9: The circuit of a unit in supercapacitor array.

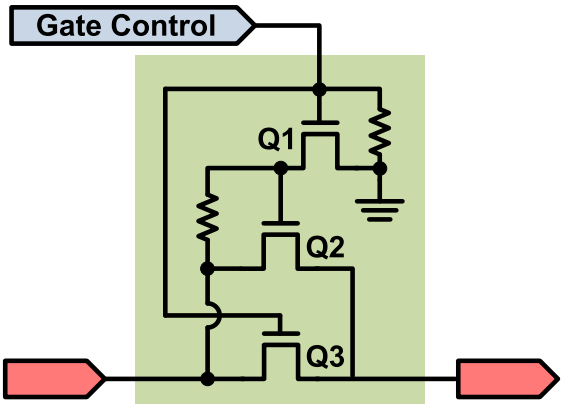

Figure 3.10: The circuit of power path switch for supercapacitor array.

both $Q1$ and $Q2$ turn on and enable the path charging to the supercapacitor. Conversely, $Q1$ and $Q2$ turn off the charging path when the gate control goes down.

Microcontroller

All functions in the DuraCap are managed and performed by a microcontroller. To save power consumption, the microcontroller uses a low voltage and a low system clock frequency.

The system requires several basic functions for the microcontroller, such as the SPI, I^2C interface, ADC, and PWM. The system uses the SPI controller to control the DAC for the I-V curve tracing. The I^2C interface is used by microcontroller to provide a communication interface with the target device. By sending commands to DuraCap via this communication interface, the target

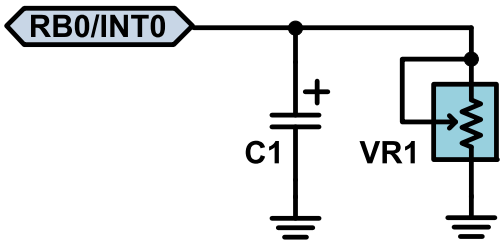

Figure 3.11: Wake-up circuit for microcontroller.

device can determine the level of available energy in each supercapacitor, hence to perform power management for the application. Note that this is an optional function for the target device. The ADC is required for the microcontroller to detect the voltage value of the solar panel, supercapacitors, and the current sensor output. Also, the PWM is necessary for the system to execute switching for the PFM regulator to perform MPPT.

Wake-Up Circuit

An important mechanism for the microcontroller to save power is to enter sleep mode. In some situations, the microcontroller does not have to be active all the time, such as at night or during bad weather conditions without sufficient sunlight, or the system is performing the bound-control MPPT. If the microcontroller is idle in most of time as is the case with many WSN applications, then it is better to enter sleep mode to avoid wasting power. In the cases given above, the microcontroller would have to wake up only once to execute the assigned procedure every couple of seconds. A long time-interval wake-up circuit can be used to generate a wake-up interrupt for the microcontroller, if it is not already supported by a built-in timer.

Fig. 3.11 shows the wake-up circuit, where $C1$ has a constant value $100\mu F$, and *VR1* is a variable resistor. In fact, the wake-up circuit is a general RC circuit with the resistor configurable. The wake-up interrupt port of the microcontroller connects to the wake-up circuit, which can be seen as open when the port is listening on the interrupt signal. The wake-up interrupt occurs

for the microcontroller while the signal changes from either 0 to 1 or 1 to 0 digitally, where the threshold voltage to identify a digital 0 or 1 is dependent on the microcontroller specification. In the DuraCap, the wake-up interrupt occurs on falling edge of the signal, i.e., while RC is discharging. To enable the wake-up function, the microcontroller must charge the capacitor before entering sleep mode, and it can easily be done by configuring the port to output a digital 1. The wake-up interrupt delay time depends on the variable resistor value in the RC circuit. In DuraCap, a programmable digital potentiometer is used, hence the micrcontroller is able to configure the resistance to control the delay time of the wake-up interrupt.

A commonly RC discharge equation is:

$$V_C(t) = \frac{q(t)}{C} = V_0 e^{-t/\tau} \tag{3.1}$$

where $\tau = RC$ is a time constant of the capacitor, t is the time during discharge, V_0 is the initial voltage of the capacitor, and V_C is the variable voltage at time t. In this thesis, we assume the threshold voltage of digital 0 is $0.22 \cdot$ *VDD*, and thus the equation becomes

$$V_C(t) = V_0 e^{-t/\tau} = 0.22 \cdot V_0 \tag{3.2}$$

$$e^{-t/\tau} = 0.22 \tag{3.3}$$

$$t = 1.5\tau \tag{3.4}$$

which means it takes 1.5τ seconds to reach $0.22 \cdot$ *VDD* during capacitor discharging. According to the cases mentioned above, the maximum wake-up delay time is 10 seconds, and thus time constant τ becomes 6.67. Then, the maximum resistance for the wake-up circuit can be calculated by the RC equation:

$$\tau = RC \Rightarrow 6.67 = \textit{VR1} \cdot C1 \tag{3.5}$$

where $C1$ is a constant value $100\mu F$, and thus the maximum resistance for the variable resistor *VR1* is $66.7k\Omega$.

Chapter 4

Implementation

Fig. 4.1 shows the DuraCap energy harvesting system. DuraCap has an area of $8.6cm \times 6.3cm$ including three supercapacitors. A Molex connector on the board connects the solar panel to the system to prevent users from plugging in reversely.

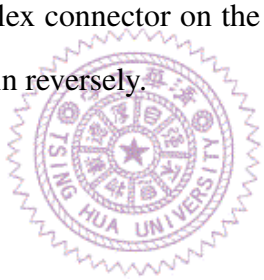

4.1 System Hardware

Solar Panel

DuraCap accepts a variety of solar panel output voltage ranging from $5.0V$ to $12.0V$, with a maximum power transfer of $6W$ to the system. In this thesis, a solar cell module is selected whose maximum output voltage and current are $6.0V$ and $200mA$, respectively. The solar panel must have the ability to produce at least the power that DuraCap needs to manage the system.

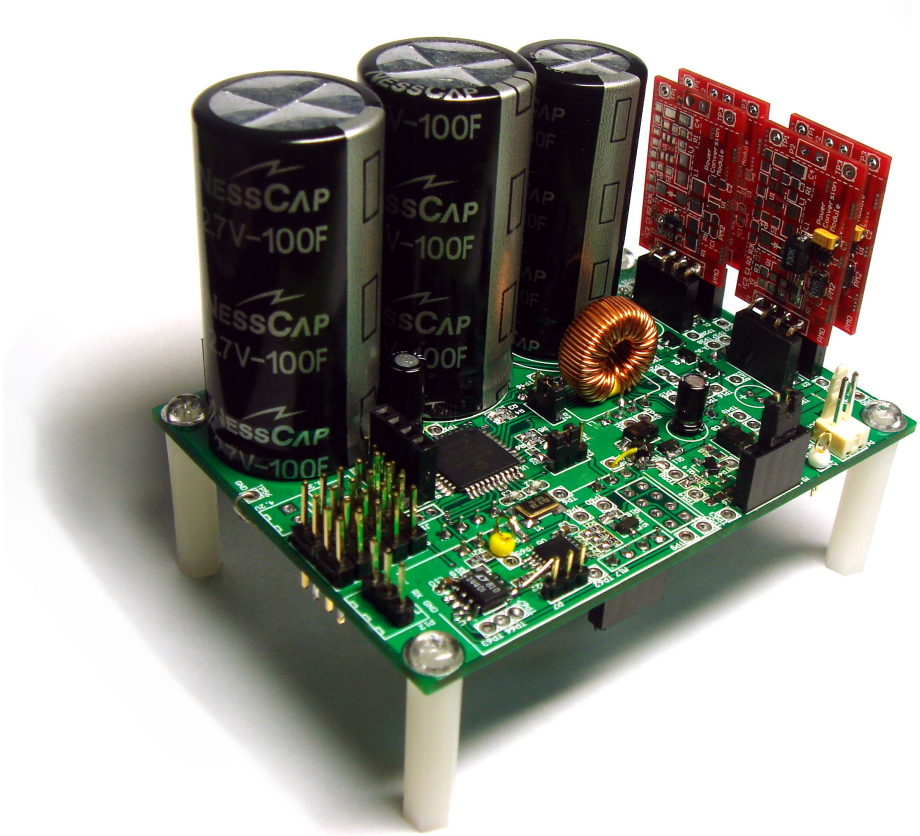

Figure 4.1: Photo of DuraCap energy harvesting system.

I-V Tracer

A DAC IC implements the I-V tracer, which can be configured through SPI as a built-in interface on the microcontroller. The DuraCap uses the Texas Instruments[19] DAC8311, which is a low power, single channel, voltage output digital-to-analog converter. The input coding to the DAC8311 is straight binary, and the ideal output voltage can be calculated by:

$$V_{OUT} = AV_{DD} \times \frac{D}{2^n} \tag{4.1}$$

where n is the DAC8311's bit resolution, which is 14, and D is the decimal value equivalent of the binary code that is set by the microcontroller. The range of D is from 0 to 16383, as derived from

$2^{14} - 1$.

The DAC8311 contains four separate modes of operation indispensable for DuraCap: normal operation, output $1k\Omega$ to *GND*, output $100k\Omega$ to *GND* and *high-z*. The DAC8311 must operate in *high-z* mode when the I-V tracer is not running to guarantee the I-V tracer does not effect the solar panel. As DuraCap performing the I-V curve tracing, the DAC8311 switches to normal mode to output the assigned voltage.

Digital Potentiometer

The variable resistor is indispensable in DuraCap, since many functions need the resistance to be changeable. Since those functions require controllability by the microcontroller, a digital potentiometer is a good solution for the system. Many different types of digital potentiometers are available in memory type and communication interface. For DuraCap, a non-volatile type with serial interface is required. Thus, the MAX5478 from Maxim-IC [9], is selected.

MAX5478 is a 256-tap, non-volatile digital potentiometer with the I^2C serial interface. The MAX5478 performs the same function as a discrete potentiometer or variable resistor, which has 256 tap points. The maximum resistance of the MAX5478 is up to $100k\Omega$ and allows the microcontroller to adjust the resistance via the I^2C. The MAX5478 contains two 256-tap non-volatile potentiometers in a single package, as shown in Fig. 4.2, which helps the system to save the area, and both potentiometers can be configured separately by the microcontroller. Furthermore, since the MAX5478 uses the I^2C interface, the microcontroller is able to connect to multiple MAX5478 units with only two pins needed, as all I^2C devices share the same data and clock bus lines.

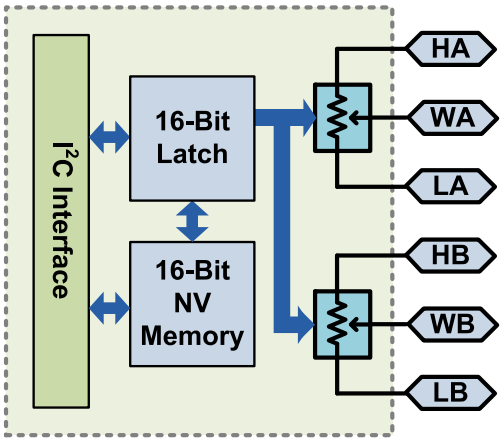

Figure 4.2: MAX5478 Block Diagarm.

Current Sensor

The current sensor is an important part in DuraCap. It measures the current output value of the solar panel so that the system can perform accurate MPPT. The DuraCap uses the MAX9928 from Maxim-IC[9], a micro-power, bidirectional current-sensor amplifier. The MAX9928 has a wide input common-mode voltage range of $-0.1V$ to $28.0V$, which is independent of supply power. It senses voltage from the R_{SENSE} and outputs a current to the other side with a ratio of $5\mu A/mV$. An external resistor converts the output current to a voltage, allowing an adjustable gain so that the voltage can be matched to the maximum ADC input of the microcontroller. The equation for the output voltage of the MAX9928 is given by:

$$V_{OUT} = (R_{SENSE} \times I_{LOAD}) \times (G_m \times R_{OUT}) \tag{4.2}$$

where I_{LOAD} is the full-scale current being sensed on R_{SENSE}, and $G_m = 5\mu A/mV$ is the transconductance of the MAX9928. The R_{OUT} can be determined by modifying the above equation to:

$$R_{OUT} = (V_{OUT})/(R_{SENSE} \times I_{LOAD} \times G_m) \tag{4.3}$$

Assuming $I_{LOAD} = 500mA$ and $V_{OUT} = 3.3V$, which depend on the maximum current being sensed and the maximum ADC input voltage, respectively, and assuming $R_{SENSE} = 0.2\Omega$, Equation 4.3 becomes:

$$R_{OUT} = (3.3V)/(0.2\omega \times 500mA \times 5\mu A/mV) \tag{4.4}$$

thus a proper resistor value of R_{OUT} can be found to be $6.6k\Omega$ for DuraCap.

Microcontroller

The DuraCap uses the Microchip [10] PIC18LF4520, an 8-bit microcontroller that is a low power and low voltage version of the PIC18F4520. PIC18LF4520 has 32 KBytes flash program memory, 1536 bytes SRAM data memory and a on-chip 256 bytes EEPROM data memory. It contains 36 GPIOs, 13-channel 10-bit ADC, PWM, UART, SPI, I^2C, an 8-bit timer, and three 16-bit timers. Two serial interfaces, SPI and I^2C, connect the digital-to-analog converter (DAC) and digital potentiometer, respectively. The analog-to-digital converter is very important, because the microcontroller relies on it to obtain the current and voltage values of the solar panel and the supercapacitors.

Supercapacitor

DuraCap uses the pseudo series supercapacitors from PAC Electronics [12]. It has a maximum voltage of $2.7V$. Totally three supercapacitors are used in DuraCap.

One of these supercapacitors is assigned as a boot supercapacitor to supply power for the system in the cold boot procedure. The boot supercapacitor in DuraCap has a smaller capacitance value of 50F, compared to others with a layout area of $18mm \times 18mm$ and $40mm$ in height. The boot supercapacitor provides a total of $182.25J$ energy for the DuraCap.

The two other supercapacitors, also known as reservoir supercapacitors, have capacitance values of 200F and provide power for both the system and the target device. They each have a layout

Table 4.1: Supercapacitors in DuraCap.

Label in Circuit	Function	Capacitance	Rated Voltage	Max. Stored Energy
$C0$	boot capacitor	$50F$	$2.7V$	$182.25J$
$C1$	supply capacitor	$200F$	$2.7V$	$729J$
$C2$	supply capacitor	$200F$	$2.7V$	$729J$

area of $22mm \times 22mm$ and $45mm$ in height. By fully charging to reservoir supercapacitors, the DuraCap can supply totally $1458J$ of energy for the target device. Table 4.1 shows a summary of supercapacitors in DuraCap.

Comparators in Bound-control Circuit

The bound-control circuit consists of four common comparators and several small components. The DuraCap uses LM339 which contains four common comparators in a single package. LM339 is a popular device since long time ago, and many famous incorporations manufacture the product LM339. In this thesis, a product of National Semiconductor[11] is chosen because it is easy to buy from a common electronic store. The National LM339 is a low power low offset quad comparator which has supply voltage in the range of $2.0V$ to $36.0V$.

Another optional device for replacement of LM339 is the TLC3704 from Texas Instruments [19]. It is a micro-power quad comparator. The TLC3704 has lower I_q of $0.02mA$ for each channel, compared to $0.2mA$ for the National LM339. The pinout of the TLC3704 is totally compatible with the LM339, and therefore the device can be replaced without any changes to the PCB.

Power

The DuraCap provides two different voltage of power supply, $3.3V$ and $4.2V$, for both the system itself and the target device. Four switching regulators are needed for these two power supplies as

Table 4.2: Regulators arrangement for two output voltage

Power Source	**4.2V**	**3.3V**
Solar Panel	LTC1779	LTC1779
Supercapacitor	LTC3400	LTC3525ESC6-3.3

shown in Fig. 3.4 in Section 3.2.3. Table 4.2 shows the arrangement of regulators in DuraCap.

LTC3525ESC6-3.3 is a micro-power, $400mA$ step-up DC-DC converter, which has $3.3V$ constant voltage output. It has high efficiency of over 90% on average. The LTC3525ESC6-3.3 has a $0.85V$ start-up voltage, which makes the input voltage range of $0.85V$ to $3.3V$. Only three small external components are required, and this helps the system reduce the needed area. In DuraCap, the LTC3525ESC6-3.3 converts the power source to $3.3V$ from a supercapacitor, which has the voltage range of $0V$ to $2.7V$.

LTC3400 is a micro-power, $600mA$ boost converter with output range of $2.5V$ to $5.0V$. The LTC3400 is placed in DuraCap to boost the voltage to up to $4.2V$ when sourving power from a supercapacitor, which has a voltage range of $0V$ to $2.7V$.

LTC1779 is a current-mode, $250mA$ step-down DC-DC converter that has a wide input range of $2.5V$ to $9.8V$. The current-mode control provides excellent AC and DC load and line regulation. The LTC1779 has an undervoltage lockout feature that shuts down the LTC1779 when the input voltage falls below $2.0V$. The DuraCap enables the LTC1779 to convert power from solar panel when the supercapacitors are empty and provides $3.3V$ of supply power for the system.

4.2 System Operation

4.2.1 Cold Boot

The DuraCap handles cold boot in the following two situations: booting up when all energy stored in the system are exhausted.

Cold booting is a procedure that starts the system from no stored energy, and it is also known as a dead start. In cold booting, the system uses the solar panel as the only power source. The only objective of the system in handling the cold boot is to charge the boot supercapacitor. The system does not deliver power to the target device when cold booting. The system exits cold booting mode after charging up the boot supercapacitor. Meanwhile, the system switches to draw the power from the boot supercapacitor and begins to charge reservoir supercapacitors.

4.2.2 Monitoring and Charging of Supercapacitor Array

The DuraCap has three supercapacitors to store energy. The system keeps monitoring the voltage of each supercapacitors all the time to decide the next function to be executed. The DuraCap first charges the boot supercapacitor as the first power source to the system. If the boot supercapacitor is exhausted, then the system searches for the second power source from either reservoir supercapacitors or the solar panel. In this case, the system first draws the power from the second and the third supercapacitors to supply power for maintaining the system. The system draws the power from the solar panel only if all energy is exhausted in the system, and then the system enters cold boot mode, which has been discussed in Section 4.2.1.

When the charging of the boot supercapacitor is completed, the system switches to normal mode in which it performs MPPT to charge the reservoir supercapacitor. In normal mode, if a supercapacitor is fully charged, then the system switches to charging the other supercapacitor no

matter how much remaining energy it has. The goal of the system in charging the supercapacitor array is to keep all supercapacitors as fully charged as possible. Henceforth, the system is able to supply durable power for the target device.

4.2.3 MPPT Operation

The MPPT in DuraCap is performed in conjunction by the solar panel I-V tracer, the microcontroller, and the bound-control circuit. The I-V tracer provides data about the solar panel to the microcontroller, and the bound-control circuit performs switching for the PFM regulator.

The system first decides the target supercapacitor to be charged. Then, the microcontroller configures the DAC in the I-V tracer to output a series of signals to vary the load on the solar panel indirectly. By performing the I-V tracing, the system obtains the maximum power point of the current solar panel.

The microcontroller calculates the upper and lower bound voltage values from the maximum power point value and configures the digital potentiometer in the bound-control circuit. After setting up the upper-bound and lower-bound voltage value for the bound-control circuit, it performs switching for the PFM regulator to operate the solar panel at the maximum power point.

DuraCap calls the I-V tracing procedure to maintain the accuracy of tracking once every ten seconds. During this ten-second interval, the microcontroller may go into the sleep mode to reduce the power consumption, if the application does not need it to execute other tasks. The ten-second wake-up interrupt to the microcontroller can be implemented by the wake-up circuit, where the delay interval is configurable by the microcontroller in the range of $0s$ to $15s$.

Chapter 5

Evaluation and Experiment

5.1 Experiment Setup

Environmental Setup

To verify the function of DuraCap, a stable and repeatable experimental environment is required. For this reason, the experiments in this chapter are performed in an indoor environment with a controllable emulated sunlight source instead of a variable sunlight in an outdoor environment. A halogen lamp is set to emulate the sunlight with a maximum light output level of over 900 lumens.

Measurement System

For experiments in this thesis, a measurement system is developed to monitor the status of the components in DuraCap. The measurement system consists of two parts: measurement hardware station and PC host measurement GUI. The measurement hardware uses the Microchip dsPIC33FJ256GP710, a high-performance DSP controller. It has a 32-channel 12-bit ADC module of up to 500k samples per second. The measurement base station transfers the measured data to

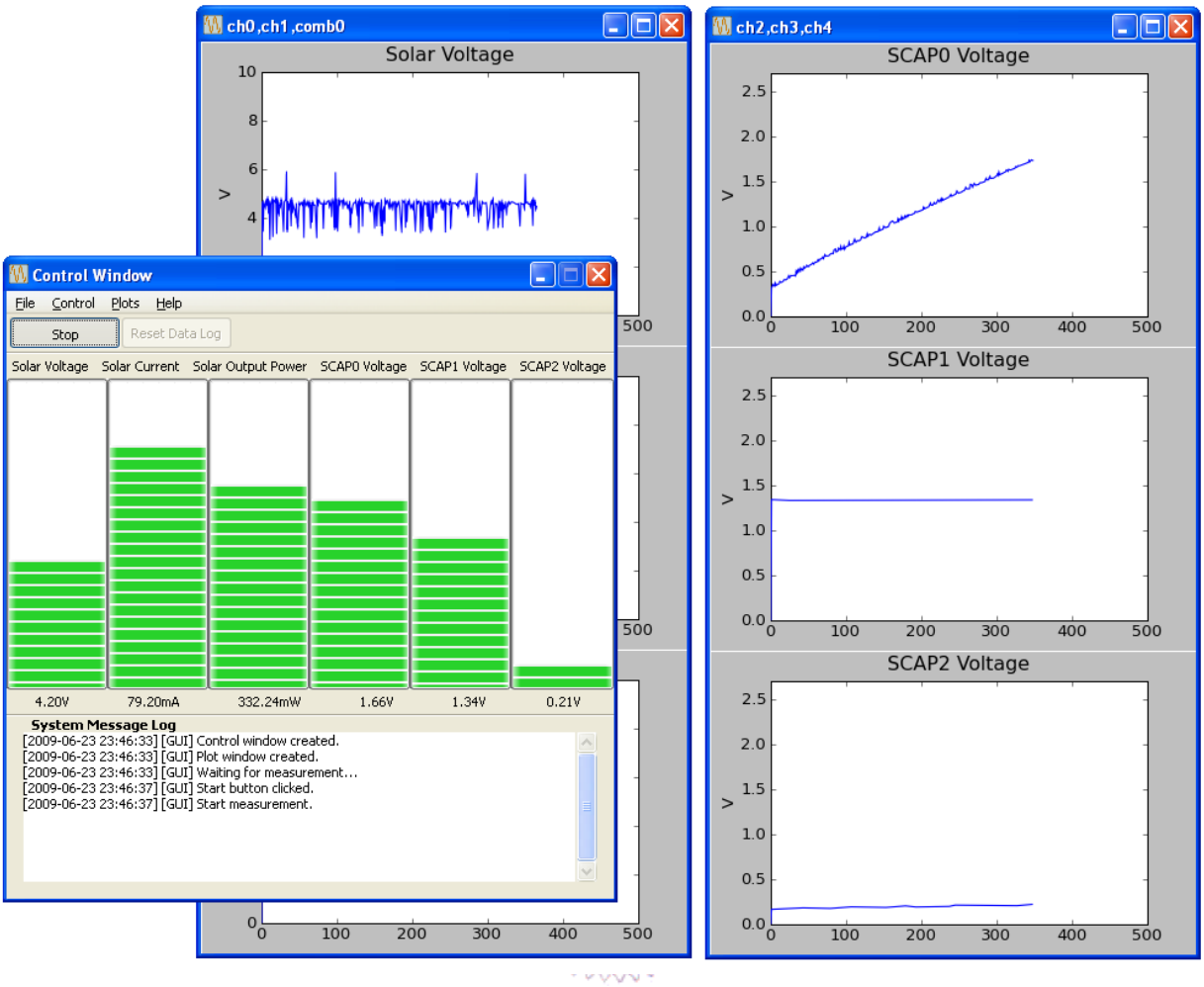

Figure 5.1: Multi-channel measurement system.

the PC host via UART at 115200 baud.

The PC host measurement GUI is developed in Python, a general-purpose high-level programming language. The channel number to be monitored is configurable by modifying the configuration file. For monitoring DuraCap, five physical channels are required, that is, one for the voltage of the solar panel V_{solar}, another for the current of the solar panel I_{solar}, and others for the supercapacitors in DuraCap. The system also supports virtual channel that can be calculated by an assigned equation, which is very helpful for monitoring the indirect data, i.e.,*(power virtual channel)* $=$ *(voltage channel)* $\times$ *(current channel)*.

The sampling rate is also configurable by the user depending on the application. Since the experimental time is long, and furthermore the response time of the supercapacitor is slow in DuraCap, the sample rate can be decreased to reduce the memory needs for the PC host.

Figure 5.1 shows a screen shot of the PC host measurement GUI.

5.2 Experimental Result

5.2.1 Enhanced Switch

The enhanced switch for DuraCap has been discussed in Section 3.2.5. The experiments presented here verify the functionality of the enhanced switch for the PFM regulator and the power path switch for the supercapacitor array in DuraCap.

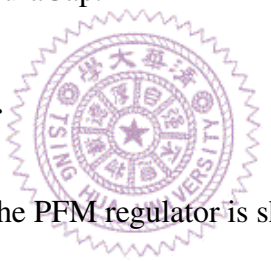

Enhanced Switch for PFM Regulator

The circuit of the enhanced switch for the PFM regulator is shown in Figure 3.8. Figure 5.2 shows the signal comparison between using and not using the enhanced switch. In Figure 5.2, *CH1* (yellow) is for the solar panel voltage V_{solar}, *CH2* (light blue) is for the gate voltage of the MOSFET V_{gs}, and *CH3* (pink) is for the control signal for the switch output from the microcontroller.

Obviously, the V_{gs} rises very slowly as shown in Fig. 5.2(a) before using enhanced switch. It has great influence on the conversion efficiency of the PFM regulator while the V_{solar} remains in the low level in most of time. By adding a diode $D1$ to the circuit of the switch in Fig. 3.8, it reduces the response time of the V_{gs}, as shown in Fig. 5.2(b), which improves the controllability to the solar panel V_{solar} and hence increases the conversion efficiency of the PFM regulator.

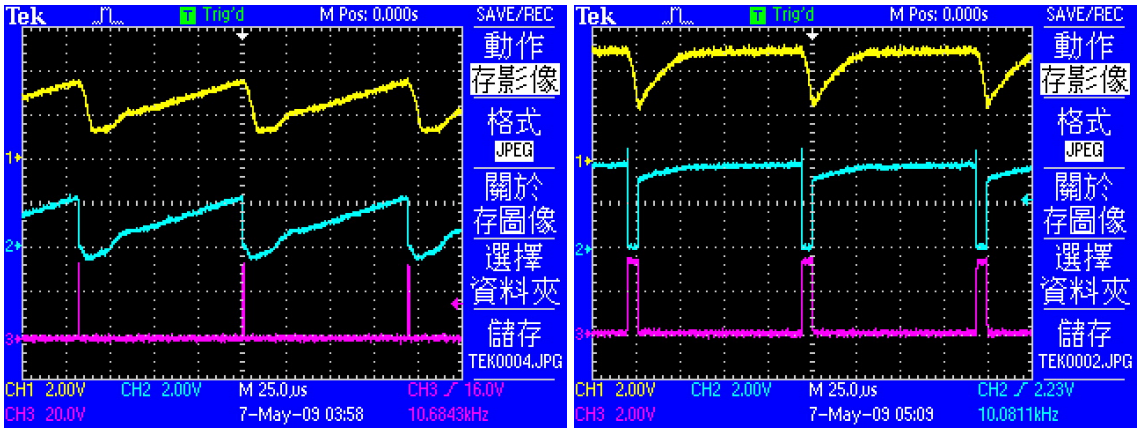

(a) Without Enhanced Switch (b) Enhanced Switch

Figure 5.2: Signal comparison between (a) without enhanced switch. (b) an enhanced switch is used for PFM regulator.

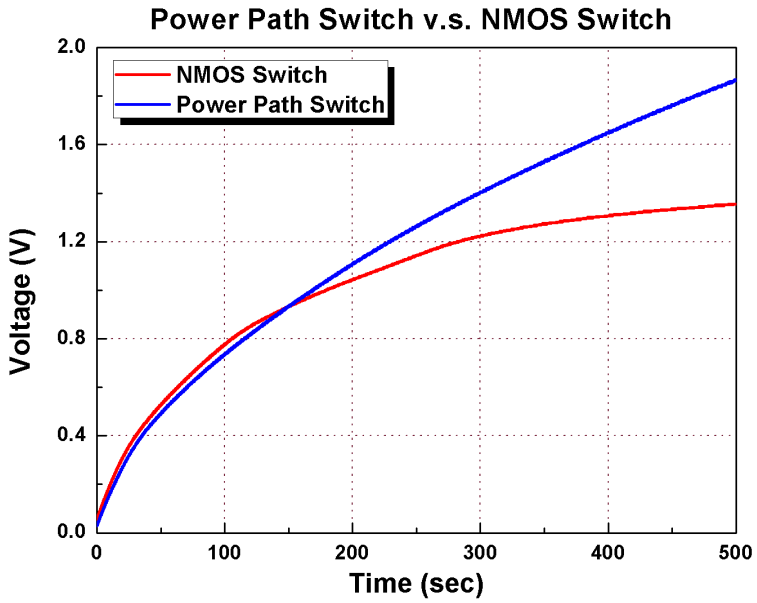

Figure 5.3: Charge curve comparison between power path swich and NMOS switch.

Power Path Switch for Supercapacitor Array

Figure 5.3 shows the charge curve comparison between using power path switch and the N-MOSFET switch. In the figure, the red line is the charge curve for the N-MOSFET switch, and

the blue line for the power path switch 5.3. When using the N-MOSFET switch, the V_{gs} becomes smaller and smaller as the voltage of the supercapacitor increasing during charge time, and then the N-MOSFET turns off while the V_{gs} is lower than V_{th}. It occurs when the supercapacitor is charged to $1.3V$.

By replacing the N-MOSFET swich with the power path switch, the charge curve appears efficiently even when the voltage of supercapacitor over $1.3V$. The circuit of power path switch for the supercapacitor array is presented in fig. 3.10.

5.2.2 I-V Curve Tracing

Th DuraCap uses I-V tracer to obtain the voltage and current curve of the solar panel, that has discussed in Section 3.2.4. In this section, an example of I-V curve tracing is presented.

Figure 5.4 shows the voltage, current, and power curves during performing I-V curve tracing by the DuraCap. The DAC outputs a linear incremental voltage signal to the gate of an N-MOSFET during I-V tracing, which controls the load of the solar panel indirectly. Since the N-MOSFET behaves linearly just in a short range of V_{gs}, the curve appears only in a short part of the captured data.

Figure 5.5 shows the I-V curve that is transformed by the result of I-V tracing in Figure 5.4. The black square shows the I-V curve of the solar panel, and the green triangle shows the P-V curve in the figure. By analyzing the P-V curve, the system can easily find the maximum power point of the solar panel, hence maintaining the high conversion efficiency for the system.

5.2.3 Charging Comparison

The DuraCap supports several MPPT approaches, including both software and hardware ones. Several MPPT approaches have been implemented and are compared with the charge time of the

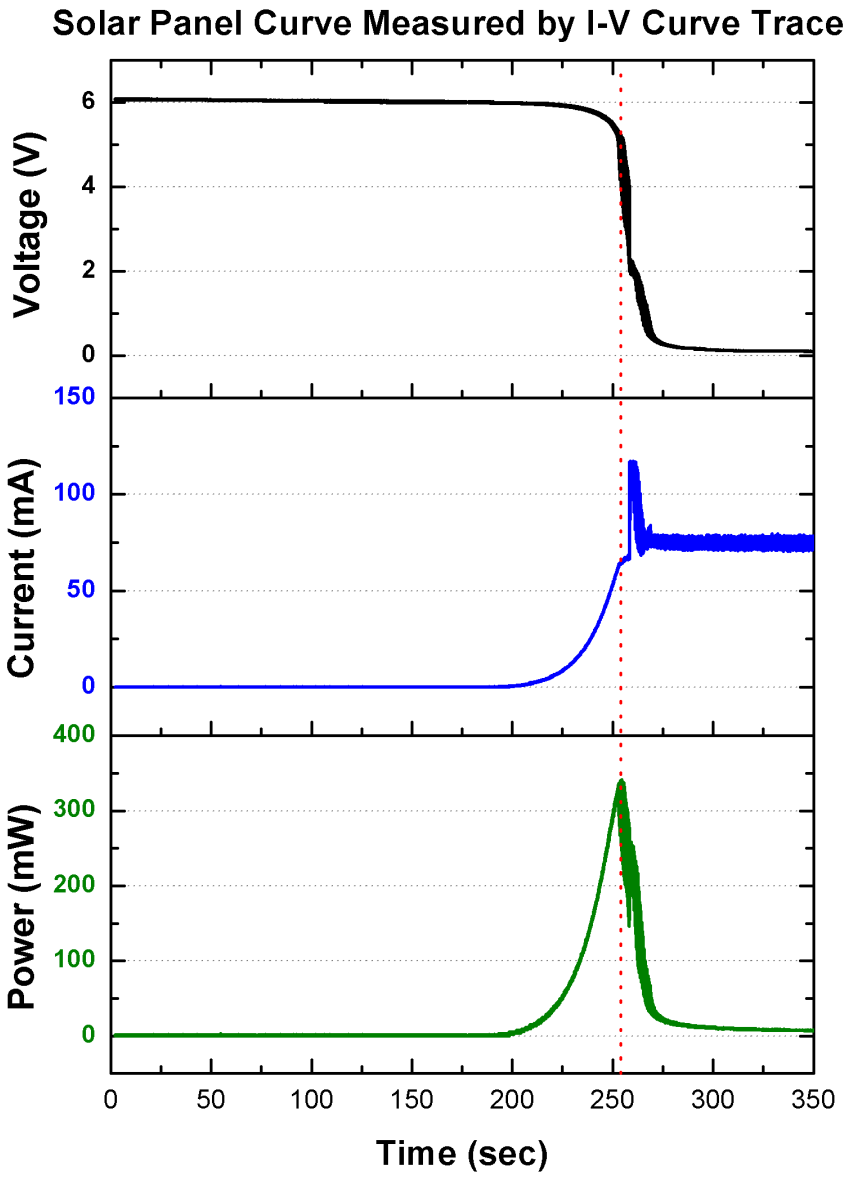

Figure 5.4: Solar panel I-V tracing performed by I-V tracer.

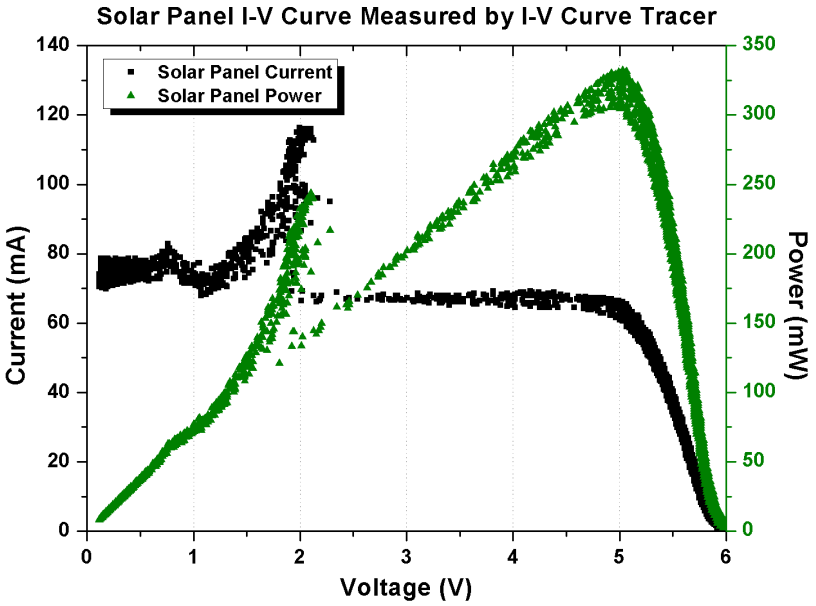

Figure 5.5: Solar panel I-V curve measured by I-V tracer.

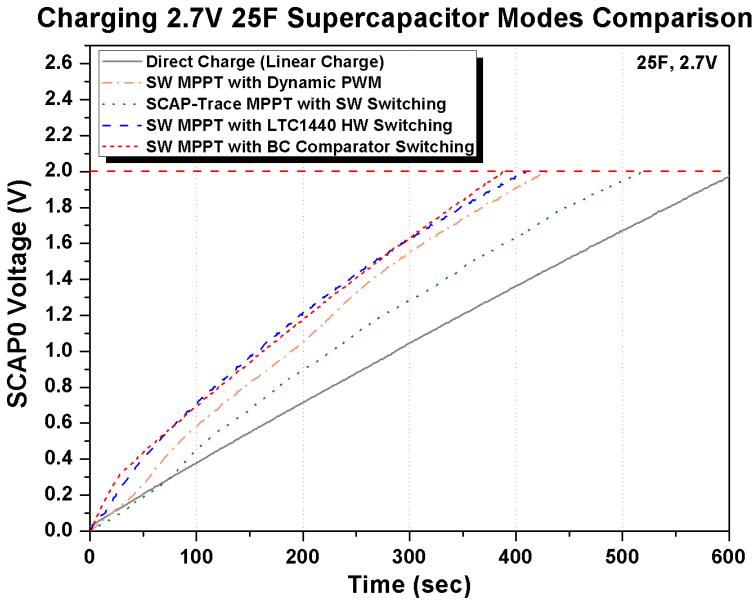

Figure 5.6: 25F supercapacitor charge time comparison.

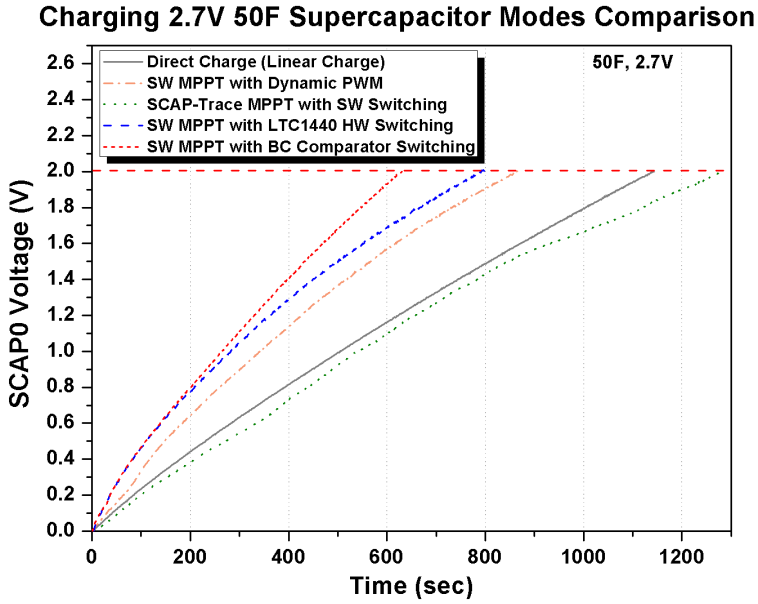

Figure 5.7: 50F supercapacitor charge time comparison.

supercapacitor.

Figure 5.6 shows the experimental result of charging the $25F$, $2.7V$ supercapacitor to $2.0V$. For linear charge, it takes 610 *seconds* to reach $2.0V$, which has the longest charge time. For both bound-control and LTC1440, it takes very closely 389 and 410 *seconds* to reach $2.0V$, respectively. It is because the principles of operation are similar between these two methods. With bound-control and the LTC1440 MPPT circuit, it allows the system to charge the supercapacitor to $2.0V$ nearly 56% faster than linear charging.

Figure 5.7 shows the experimental result of charging the $50F$, $2.7V$ supercapacitor to $2.0V$. This time, the bound-control MPPT takes the shortest charge time to reach $2.0V$. The bound-control MPPT takes 631 *seconds*, which is 25% faster than the LTC1440 MPPT ($791s$) and 81% faster than linear charging ($1145s$).

Figure 5.8 and Table 5.1 summarize the charging time for each MPPT approach. It is obvi-

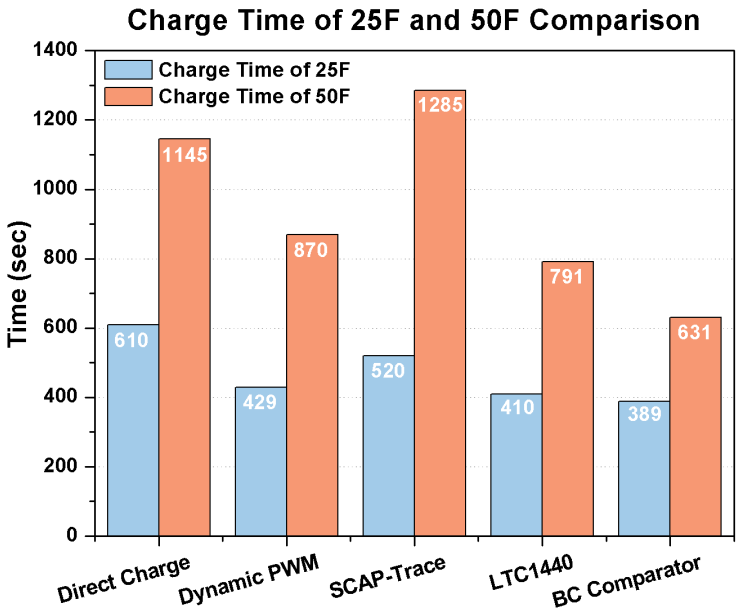

Figure 5.8: 25F v.s. 50F charge time comparison.

Table 5.1: 25F v.s. 50F charge time comparison

Supercapacitor	**Linear Charge**	**Dynamic PWM**	**Supercapacitor Tracing**	**LTC1440 MPPT**	**Bound-Control MPPT**
$25F, 2.0V$	$610s$	$429s$	$520s$	$410s$	$389s$
$50F, 2.0V$	$1145s$	$870s$	$1285s$	$791s$	$631s$

ously that the linear charge is the most inefficient method to charge the supercapacitor, and the supercapacitor-tracing takes 1285 *seconds* to charge $50F$ supercapacitor to $2.0V$, which is slower than linear charge, indicating that it is an inefficient approach as the capacitance of the supercapacitor increases. The bound-control circuit appears to be the most efficient MPPT approach in DuraCap to charge the supercapacitor.

Chapter 6

Conclusion

In this thesis, an energy harvesting system DuraCap is presented. The DuraCap provides durable power for applications in wireless sensor network that extends the life time from several months to tens of years. The cold boot feature on the DuraCap ensures that the system is able to recover rapidly from total exhaustion of stored energy. We have developed a bound-control PFM regulator controller for MPPT, which allows the system to maintain the maximum power level that can be transferred from the solar panel. The DuraCap contains three supercapacitors to store energy. The system charges the supercapacitor by using a PFM regulator that significantly increases the conversion efficiency. An I-V tracer is implemented in DuraCap to obtain the characteristic of the solar panel, such that the system is able to self-configure to match different solar panel automatically. An enhanced switch for the PFM regulator and a power path switch for the supercapacitor array are designed for low-voltage control, which helps the system to reduce the power consumption.

Appendix A

Schematics

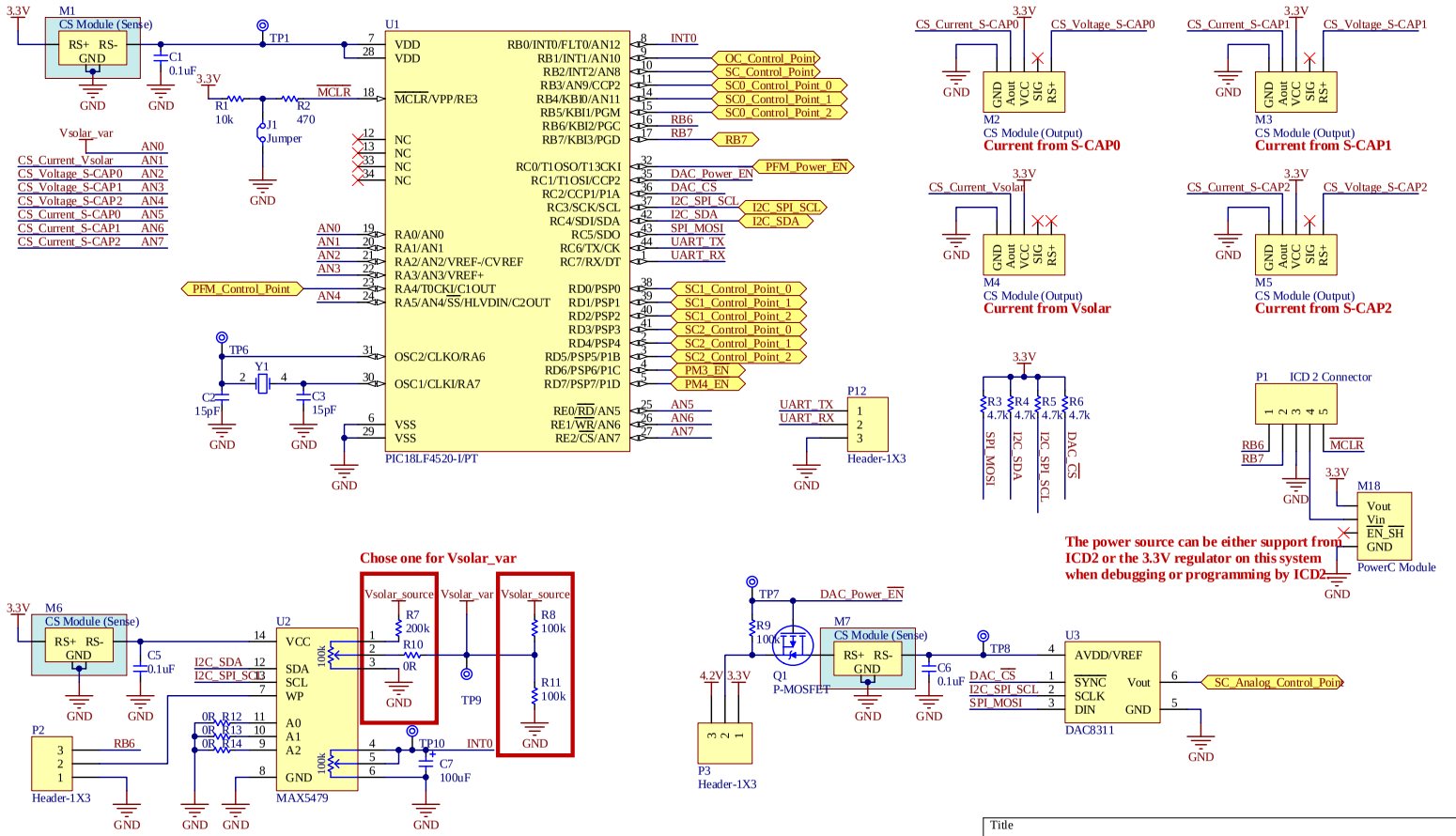

Title		
Size A4	Number	Revision
Date: 2009/6/25		Sheet of
File: D:\Protel Today (20090302)\..\Solar Maximum Power Point Controller.SchDoc		Drawn By:

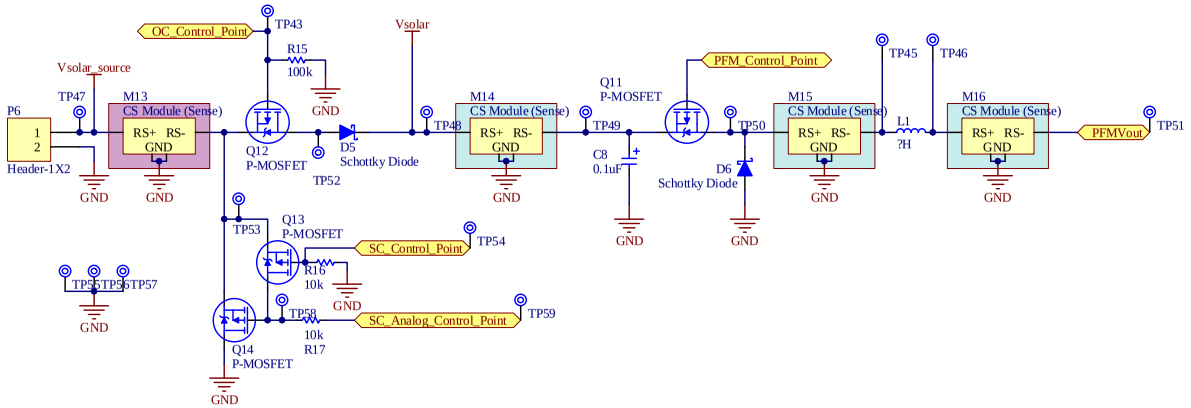

Title		
Size: A4	Number	Revision
Date: 2009/6/25		Sheet of
File: D:\Protel Today (20090302)\..\Solar Power Source 1\PFM Circuit.SchDoc		Drawn By:

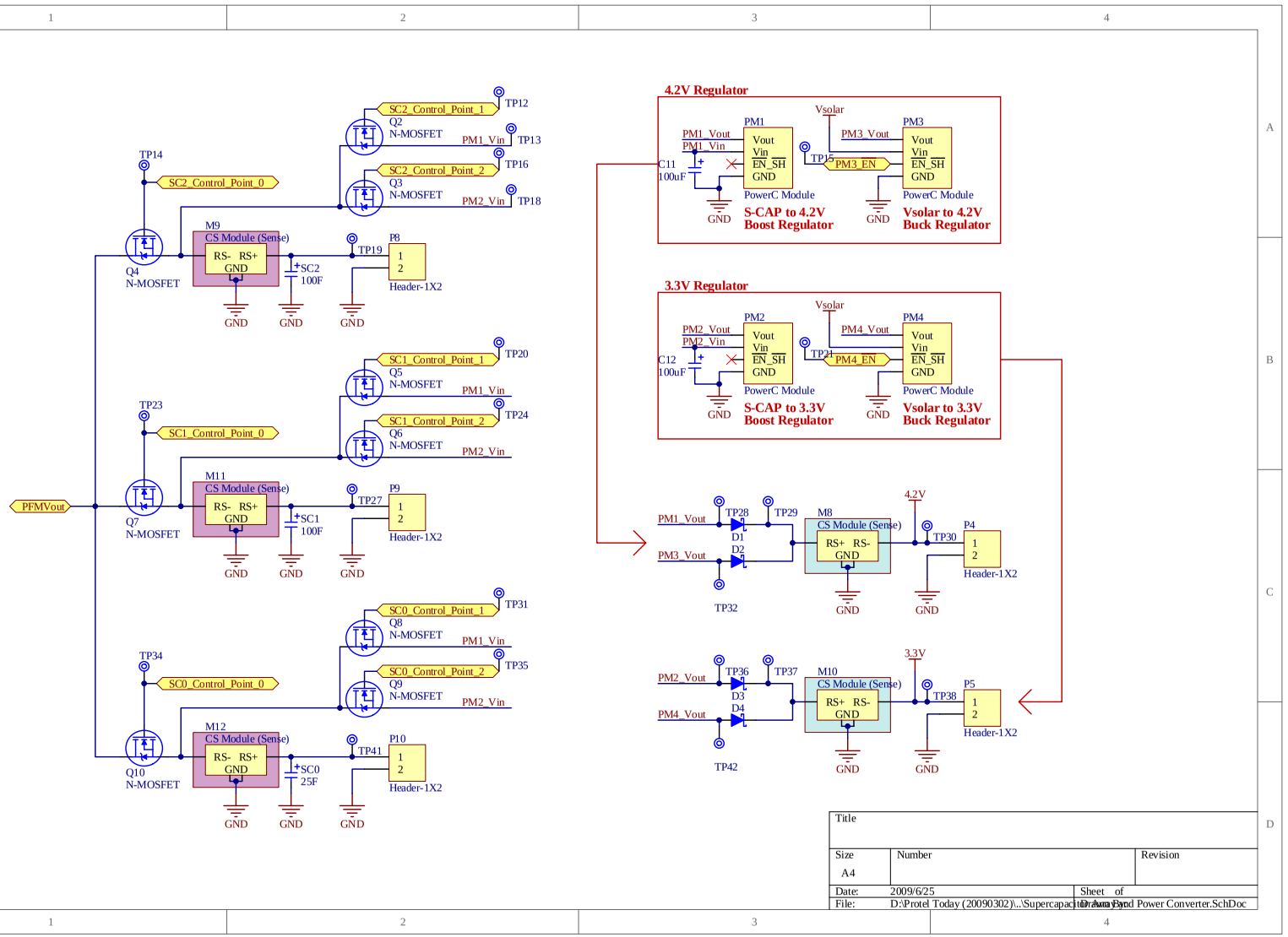
4.2V Regulator
PM1
Vout
Vin
EN_SH
GND
PowerC Module
S-CAP to 4.2V
Boost Regulator
PM3
Vsolar to 4.2V
Buck Regulator
3.3V Regulator
PM2
PM4
S-CAP to 3.3V
Boost Regulator
Vsolar to 3.3V
Buck Regulator
PM1_Vout
PM1_Vin
PM2_Vout
PM2_Vin
PM3_Vout
PM4_Vout
PM3_EN
PM4_EN
C11
100uF
C12
100uF
TP15
TP33
SC2_Control_Point_1
SC2_Control_Point_0
SC2_Control_Point_2
SC1_Control_Point_1
SC1_Control_Point_0
SC1_Control_Point_2
SC0_Control_Point_1
SC0_Control_Point_0
SC0_Control_Point_2
Q2
Q3
Q4
Q5
Q6
Q7
Q8
Q9
Q10
N-MOSFET
M9
M11
M12
CS Module (Sense)
RS- RS+
GND
SC2
100F
SC1
100F
SC0
25F
P8
P9
P10
Header-1X2
PFMVout
TP12
TP13
TP14
TP16
TP18
TP19
TP20
TP23
TP24
TP27
TP31
TP34
TP35
TP41
M8
M10
D1
D2
D3
D4
P4
P5
4.2V
3.3V
TP28
TP29
TP30
TP32
TP36
TP37
TP38
TP42
Title
Size
A4
Number
Revision
Date:
2009/6/25
Sheet of
File:
D:\Protel Today (20090302)\...\Supercapacitor Energy Power Converter.SchDoc
Drawn By:

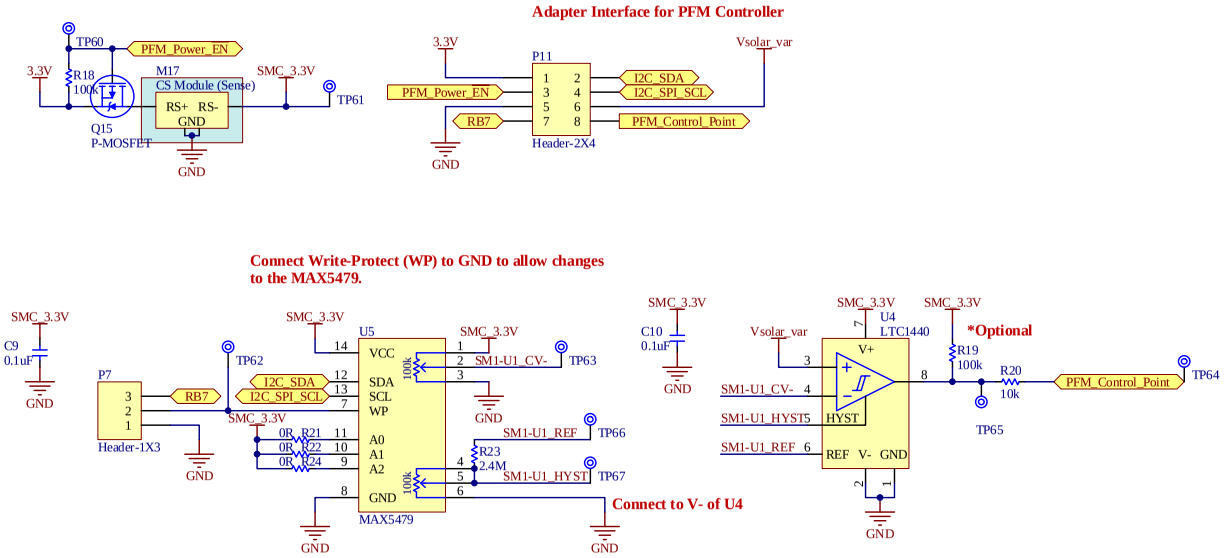

Title		
Size: A4	Number	Revision
Date: 2009/6/25	Sheet of	
File: D:\Protel Today (20090302)\...\Solar MPP Controller(LTC1440).SchDoc	Drawn By:	

Bibliography

[1] BRUNELLI, D., BENINI, L., MOSER, C., AND THIELE, L. An efficient solar energy harvester for wireless sensor nodes. In *DATE '08: Proceedings of the conference on Design, automation and test in Europe* (New York, NY, USA, 2008), ACM, pp. 104–109.

[2] CHULSUNG PARK, CHOU, P. Ambimax: Autonomous energy harvesting platform for multi-supply wireless sensor nodes. In *SenSys '05: Proceedings of the 3rd international conference on Embedded networked sensor systems* (New York, NY, USA, 2006), Institute of Electrical and Electronics Engineers Inc., pp. 309–309.

[3] FARANDA, R., AND LEVA, S. A comparative study of mppt techniques for pv systems. In *AEE'08: Proceedings of the 7th WSEAS International Conference on Application of Electrical Engineering* (Stevens Point, Wisconsin, USA, 2008), World Scientific and Engineering Academy and Society (WSEAS), pp. 100–105.

[4] FARMER, J. R. A comparison of power harvesting techniques and related energy storage issues. Master's thesis, Virginia Polytechnic Institute and State University, 2007.

[5] JIANG, X., POLASTRE, J., AND CULLER, D. Perpetual environmentally powered sensor networks. In *Information Processing in Sensor Networks, 2005. IPSN 2005.* (2005), IPSN, pp. 463–468.

[6] KRISHNA, M. Powering telecommunications network interfaces using photovoltaic cells and supercapacitors. In *Journal of Technology and Business (JTB)* (2007), pp. 73–84.

[7] LI-QUN, L., AND ZHI-XIN, W. A rapid mppt algorithm based on the research of solar cell's diode factor and reverse saturation current. *WTOS 7*, 5 (2008), 568–579.

[8] LIN, K., YU, J., HSU, J., ZAHEDI, S., LEE, D., FRIEDMAN, J., KANSAL, A., RAGHUNATHAN, V., AND SRIVASTAVA, M. Heliomote: enabling long-lived sensor networks through solar energy harvesting. In *SenSys '05: Proceedings of the 3rd international conference on Embedded networked sensor systems* (New York, NY, USA, 2005), ACM, pp. 309–309.

[9] MAXIM. Maxim integrated products. http://www.maxim-ic.com/, 2009.

[10] MICROCHIP. Microchip technology inc. http://www.microchip.com/, 2009.

[11] NATIONAL. National semiconductor inc. http://www.national.com/, 2009.

[12] PAC. Pac electronics inc. http://www.pactw.com.tw/, 2009.

[13] RAGHUNATHAN, V., KANSAL, A., HSU, J., FRIEDMAN, J., AND SRIVASTAVA, M. Design considerations for solar energy harvesting wireless embedded systems. In *IPSN '05: Proceedings of the 4th international symposium on Information processing in sensor networks* (Piscataway, NJ, USA, 2005), IEEE Press, p. 64.

[14] S., D. Basics of design: Battery power management. In *Supplement to Electronic Design* (2004).

[15] SHAO, H., TSUI, C.-Y., AND KI, W.-H. An inductor-less mppt design for light energy harvesting systems. In *ASP-DAC '09: Proceedings of the 2009 Conference on Asia and South Pacific Design Automation* (Piscataway, NJ, USA, 2009), IEEE Press, pp. 101–102.

[16] SIMJEE, F., AND CHOU, P. H. Everlast: long-life, supercapacitor-operated wireless sensor node. In *ISLPED '06: Proceedings of the 2006 international symposium on Low power electronics and design* (New York, NY, USA, 2006), ACM, pp. 197–202.

[17] SIMJEE, F., SHARMA, D., AND CHOU, P. H. Everlast: long-life, supercapacitor-operated wireless sensor node. In *SenSys '05: Proceedings of the 3rd international conference on Embedded networked sensor systems* (New York, NY, USA, 2005), ACM, pp. 315–315.

[18] SMITH, T., MARS, J., AND TURNER, G. Using supercapacitors to improve battery performance. In *Power Electronics Specialists Conference, 2002. pesc 02. 2002 IEEE 33rd Annual* (2002), IEEE, pp. 124–128 vol.1.

[19] TI. Texas instruments incorporated. http://www.ti.com/, 2009.